Theoretical Model of the Bistable Semiconductor Laser Diode Based on the Rate Equations

Vítězslav JEŘÁBEK[1], *Ivan HÜTTEL*[2]

[1]Department of Microelectronics, CTU FEE, Technicka 2, 166 27, Prague 6, Czech Republic
[2]Institute of Chemical Technology, Technicka 5, 166 28, Prague 6, Czech Republic

jerabek@fel.cvut.cz, Ivan.Huttel@vscht.cz

Abstract. *The paper describes theoretical and experimental results that enabled the authors to proof optical bistability behavior of a specially modified bistable semiconductor laser diode (BLD) created on a structure with a saturable absorption section. A mathematical model of the light-current characteristic, condition for bistability and the basic parameters of the hysteresis loop were derived by solving a system of three rate equations. That system was used for simulation of the light-current characteristic and conditions of bistability of the realized BLDs. For selected operating points of the simulated light-current characteristic the parameters of hysteresis loop and element values of the BLD electrical equivalent circuit for small signal variations were calculated. The bistability was experimentally measured by the new time method devised for impulse bistability verification (IBV). The basic measured and calculated parameters of the hysteresis loop of the BLD light-current characteristic were compared.*

Keywords

Optical bistability, bistable semiconductor laser diode, rate equation.

1. Introduction

Recently, in the realm of integrated optoelectronics appear devices exploiting new principles. One of them is the bistable semiconductor laser diode (BLD), utilizing the effect of absorption-based optical bistability. Optical bistability is one of the effects that were first forecast and only later observed. Lasher attracted attention to optical bistability in 1964 [1] and it was confirmed experimentally by Basov in 1968 [2].

The absorption-based optical bistability of the multisection laser diode (LD) belongs to the nonlinear dynamic optical phenomena in LD radiation that are based on Q switching [3]. This physical mechanism is a result of nonlinear dependence of the absorption and gain coefficients of the absorbing and gain region of the divided active layer of the semiconductor LD and manifests itself in the LD radiation as self-pulsations or optical bistability. A few years ago several papers were published describing the origin of bistability in LDs comprising a double heterostructure that was purposefully modified by dividing the stripe contact for achieving the bistable mode. The papers differed in semiconductor types, ways of strip contact splitting and also according to physical mechanism of bistability [4], [5] and [7].

An important dependence expressing the bistable properties of the BLD is its transmission characteristic (light-current characteristic). Its analytic expression can be derived by solving three rate equations. The BLD transmission characteristic was theoretically and experimentally determined in [7], [8] and [9]. If we rewrite the sentence with proper ordering, it is possible to derive the principal condition for bistability appearance as well as the conditions necessary for the creation of pulsations in the LD radiation [10], [11].

This article deals with theoretical results and experiments that enabled the authors to mathematically and experimentally describe bistability of a specially modified double heterostructure $Ga_{1-x}Al_xAs/GaAs$ LD with a saturable absorption section (see Section 2). The mathematic model of the light-current characteristic was derived by static solution of the rate equation and it was used to simulate the characteristics of the realized BLDs. The characteristics obtained by the numerical modeling were optimized according to the measurement results. Numerical values parameters of the BLD linear equivalent circuit for small signal variations were calculated for selected operating points of the simulated light-current characteristics.

To prove the bistability of the BLD a IBV method is proposed. Using this method, the principal parameters of the hysteresis loop in the light-current characteristic for the realized BLD samples are determined.

2. Realization and Measurement of the BLD

The double heterostructure (DH) laser diode with a split contact on the top p-side was realized by a standard

LPE (liquid phase epitaxy) process in our laboratory. Typical doping levels are given in Fig. 1. The device was realized in a classical ternary DH $Ga_{1-x}Al_xAs/Ga_{1-y}Al_yAs/GaAs$ where x=0.4, y=0.1 and with multiple-divided stripe contact.

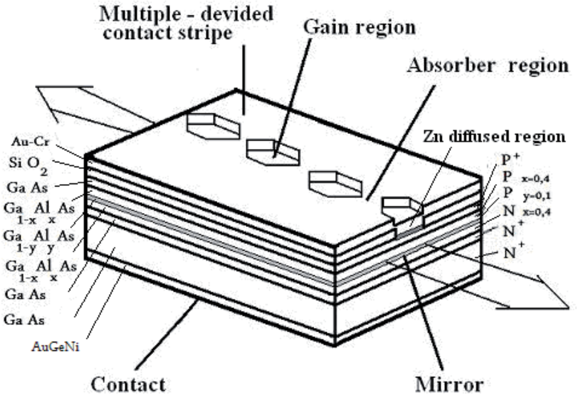

Fig. 1. $Ga_{1-x}Al_xAs/ Ga_{1-y}Al_yAs/GaAs$ double heterostructure with multiple-divided stripe contact.

The strip contact masking was arranged according to [5]. The distance between contact islets was increased from 10 to 20 μm. The axial length of the contact islet was 30 μm and width 10 μm (see Fig. 1).

To prove bistability, measurements were carried out during the first stage of work selecting only samples showing bistability. All the selected BLD samples operated in the impulse regime only. Because a BLD is a sequential device whose internal state depends on the amplitude and timing of driving pulses, the bistable behavior was verified by the method of gradual setting and resetting the device by a set of current pulses and observing the radiation response timing of the BLD by the IBV method. The block diagram of the measuring system is shown in Fig. 2.

To demonstrate bistability, two synchronized power pulse generators G1 and G2 were used. The output pulses from both generators were combined in a power divider, separating the outputs of both generators. Generator G1 provided the fundamental current pulse, setting the operating point of the BLD. This generator was synchronized with a dual-output generator G2, providing the set and reset pulses. The BLD was placed in a 50 Ω wave impedance coaxial head and connected to a coaxial modulation line. The time response of the driving impulse was determined by a current probe. The radiation propagates from the BLD through the optical system to a fast photodiode. The pulse response from the photodiode is monitored by a sampling oscilloscope equipped with a plotter. A set of driving current impulses and the corresponding radiation time responses that describe the light-current impulse characteristics of the BLD are shown in Fig. 3. At time points T_1 and T_2 the setting and resetting pulses were generated. It is clear from Fig. 3 that transition from a lower to a higher radiation level depends on the amplitude of the driving current impulses. The amplitudes of the current pulses and the magnitude of the radiation transition from the lower to the higher level were used to determine the static and dynamic parameters of the BLD hysteresis loop, used as initial values for the light-current characteristic simulation.

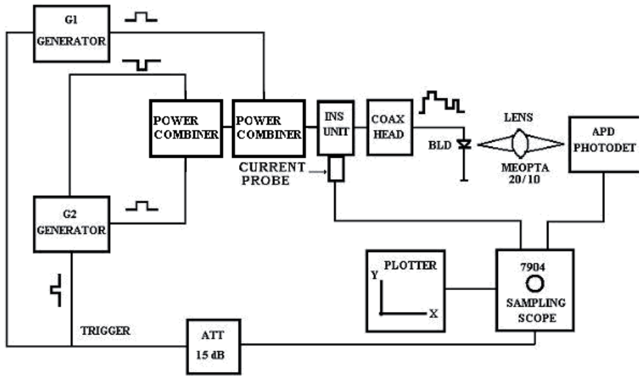

Fig. 2. Block diagram of pulse method for bistability verification IBV.

The knowledge of the waveforms enabled us to determine the BLD impulse light-current characteristic and the basic parameters of the hysteresis loop (see Fig. 6, Tab. 3).

Also the temperature dependence of the pulsed light-current characteristic was found. For this purpose a system for integral light-current characteristic measurement was used, recording the monitored optical output power on drive pulse current and temperature.

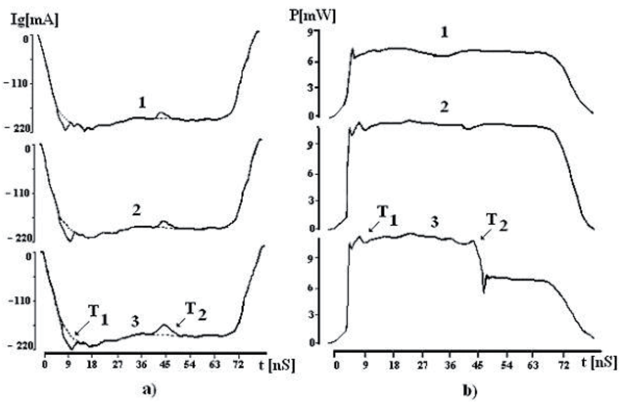

Fig. 3. The waveforms a) represent the BLD driving current pulses, the waveforms b) represent the optical output (T_1 and T_2 are setting and resetting times) [6].

The bistable characteristic depends on device temperature in the range of thirty degrees. The BLD threshold current values were I_{gth} = 140 to 220 mA and hysteresis width ΔI_{gh} = 5 to 10 % I_{gth}. The sizes of discontinuous jumps of the optical output were ΔP_l = 0.5 to 3.5 mW, see Tab. 3. The transition times between the stable states were t_r = 0.5 to 1 ns, t_f = 3 ns. The amplitudes of the current pulses and the magnitude of the radiation transition from the lower to the higher level were used to determine the static and dynamic parameters of the BLD hysteresis loop, used as initial values for measured and simulated the light-current characteristic, shown in Fig. 6.

3. Mathematical Model Using the Rate Equations

In this section a mathematical model of the light-current characteristics is derived and was justified by comparison to the experimentally measured data obtained by BIV method. The model was based on the set of the rate equations [4]. We analyzed the stationary solution of the three rate equations system from [4]. The first equation was formulated for the density of minority carriers in the gain section (1), the second one for those in the absorbing section (3) and the third one for the density of photons in the lasing mode (5). Measurements show that, when this laser is based for stable operation, the light is emitted into one longitudinal mode. This simple optical behavior can be modeled by one rate equation for the density of photons in the lasing mode. The carrier and photons densities have been averaged over the length of the device. The three equations are given (1), (3) and (5),

$$\frac{dN_g}{dt} = \frac{I_g}{eV_g} - g_g\left(N_g - N_{og}\right)N_{ph} - \frac{N_g}{\tau_g} \tag{1}$$

where

$$\frac{1}{\tau_g} = B_g\left(N_g + N_k\right), \tag{2}$$

$$\frac{dN_a}{dt} = \frac{I_a}{eV_a} - g_a\left(N_a - N_{oa}\right)N_{ph} - \frac{N_a}{\tau_a} \tag{3}$$

where

$$\frac{1}{\tau_a} = B_a\left(N_a + N_k\right), \tag{4}$$

$$\frac{dN_{ph}}{dt} = g_g\alpha_1\left(N_g - N_{og}\right)N_{ph} + g_a\alpha_2\left(N_a - N_{oa}\right)N_{ph} + $$
$$+\beta\left[\alpha_1 B_g\left(N_g + N_k\right)N_g + \alpha_2 B_a\left(N_a + N_k\right)N_a\right] - \frac{N_{ph}}{\tau_{ph}}. \tag{5}$$

Here N_g is the density of carriers in the gain region and N_a are the corresponding variables in the absorption region, N_{ph} is the photon density in the lasing mode, N_{og}, N_{oa} and N_o are the carriers density required for transparency in generation or absorption regions, N_k is the doping concentration of the active region, g_g, g_a is the gain constant in generation and absorption region. The linear gain dependence on the injected carrier density $G(N) = g(N - N_0)$ is used after [4], τ_{ph} is the photon lifetime and β is the coupling coefficient for spontaneous emission into the lasing mode. Since the carrier densities vary over a large range, we use in the model bimolecular recombination rate, where B_g, and B_a are the recombination constant for bimolecular spontaneous transitions, where life time of the carriers were describe by (2) and (4). I_g and I_a is the current injected into gain and absorption section, $V_g = \alpha_1 V$, $V_a = \alpha_2 V$ are the volumes of the generation and absorption regions, where $\alpha_1 + \alpha_2 = 1$.

We analyzed the stationary solution of equation (1) – (5). in [6]. The light-current characteristics given by (7), (8) and (9) were derived from the static solution of the rate equations under condition (6):

$$\frac{dN_g}{dt} = \frac{dN_a}{dt} = \frac{dN_{ph}}{dt} = 0\,. \tag{6}$$

The static solutions of the rate equations are parametric quadratic system $I_g = f_1(N_{ph}, N_g)$, $N_g = f_2(N_{ph}, N_a)$ and $N_a = f_3(N_{ph})$, where we assume $I_a = 0$. A parameter of the system (7), (8), (9) is α_2 / α_1.

$$I_g = eV_g B_g\left[N_g{}^2 + \left(\frac{g_g}{B_g}N_{ph} + N_k\right)N_g - \frac{g_a N_0}{B_g}N_{ph}\right], \tag{7}$$

$$N_g = -\left(\frac{g_g}{2B_g\beta}N_{ph} + \frac{N_k}{2}\right) \pm$$
$$\pm\left[\left(\frac{g_g}{2B_g\beta}N_{ph} + \frac{N_k}{2}\right)^2 - \frac{\alpha_2 B_a}{\alpha_1 B_g}\left\{N_a^2 + \left(\frac{g_a}{\beta B_a}N_{ph} + N_k\right)N_a\right\} + \frac{g_g N_{gp}}{\beta B_g}N_{ph}\right]^{1/2}, \tag{8}$$

$$N_a = -\left(\frac{g_a}{2B_a\beta}N_{ph} + \frac{N_k}{2}\right) \pm \left[\left(\frac{g_a}{2B_a\beta}N_{ph} + \frac{N_k}{2}\right)^2 + \frac{gN_{oa}}{B_a}N_{ph}\right]^{1/2}. \tag{9}$$

For a graphical presentation of the results we use the following normalization (10), (11):

$$I_{gth} = eV_g B_g\left[N_{og} + \frac{g_a\alpha_2}{g_g\alpha_1}N_{oa} + \frac{1}{\alpha_1 g\tau_{ph}}\right]\left[N_{og} + \frac{g_a\alpha_2}{g_g\alpha_1}N_{oa} + \frac{1}{\alpha_1 g\tau_{ph}} + N_k\right] \tag{10}$$

$$N_{phs} = \left(g_a\tau_a\right)^{-1}. \tag{11}$$

A calculated light-current characteristic is shown in Fig. 4.

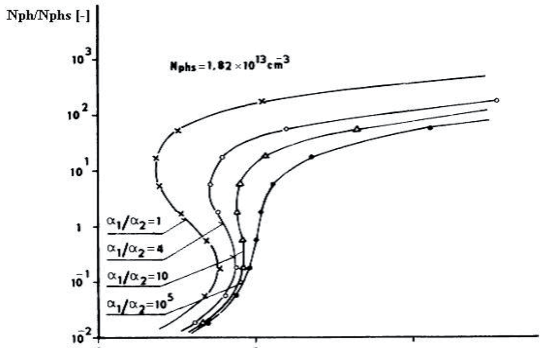

Fig. 4. Normalized static light-current characteristics with parameter α_1/α_2.

The physical constants were determined by dynamic method measuring of the cut-off frequency of the modulation characteristic of a LD, excited below the threshold and by measuring frequency of the photon-electron resonance of samples excited above the threshold. A LD was prepared by identical technology, but without absorption regions. The values of the physical constants were optimized throughout the simulation process, see Tab. 1.

g [cm^3·s^{-1}]	N_0 [cm^{-3}]	τ_{ph} [s]	B [cm^3·s^{-1}]
8·10^{-6}	2.15·10^{18}	1.5·10^{-12}	1.3·10^{-10}
V [cm^3]	N_k [cm^{-3}]	β [-]	α_2 / α_1 [-]
1.5·10^{-9}	5.9·10^{17}	10^{-4}	0.25

Tab. 1. Optimized values of the physical constants for light-current characteristic modeling and the BLD electrical small signal equivalent circuit.

4. The Small Signal Equivalent Circuit of the BLD

An equivalent electrical small signal circuit for the BLD in Fig. 5 was derived for selected operating points A, B and D on the simulated light-current characteristics shown in Fig. 6. The element values of the circuit are specified in Tab. 2.

	C_g[nF]	R_g[Ω]	C_a[nF]
P$_1$	7.9	0.16	7
P$_2$	7.3	0.14	1.1
P$_{max}$	6.7	0.05	1.8
	L [pH]	R_s [mΩ]	K_1 [-]
P$_1$	4.4	2006	1.120
P$_2$	0.27	1.3	0.970
P$_{max}$	0.07	0.03	0.530

Tab. 2. The element values of a BLD equivalent electrical small signal circuit.

This circuit is described by a set of circuit equations (12) through (14), which are obtained from small signal analysis of equations (1) to (3) according to [4]. Based on the electrical equivalent circuit knowledge the radiation stability of a semiconductor LD can be analyzed or derived the signal drivers aimed at suppressing the unwanted dynamic effects in the radiation response of a LD or BLD, respectively.

$$\frac{du_g}{dt} = \frac{1}{C_g}\left(i_g - \frac{u_g}{R_g}\right) - i_L, \qquad (12)$$

$$\frac{du_a}{dt} = \frac{1}{C_a}\left(i_a - \frac{u_a}{R_a} + K_1 i_L\right), \qquad (13)$$

$$\frac{di_L}{dt} = \frac{1}{L}\left(u_g + N_1 u_a - R_s i_L\right) \qquad (14)$$

where

$$R_g = \left[C_g\left(\frac{1}{\tau_g} + g_g \bar{N}_{ph}\right)\right]^{-1}, \qquad (15)$$

$$R_a = \left[C_a\left(\frac{1}{\tau_a} + g_a \bar{N}_{ph}\right)\right]^{-1}, \qquad (16)$$

$$C_g = \frac{e^2 V_g \bar{N}_g}{m_g kT}, \qquad (17)$$

$$C_a = \frac{e^2 V_a \bar{N}_a}{m_a kT}, \qquad (18)$$

$$L = \left[C_g \alpha_1 g\left(\bar{N}_g - N_{og}\right)\left(\frac{\beta}{\tau_g} + g_g \bar{N}_{ph}\right)\right]^{-1}, \qquad (19)$$

$$R_s = L\left(\alpha_1 g_g \frac{I_{gth}\tau_g}{eV_g} - \alpha_1 g_g \bar{N}_g - \alpha_2 g_a \bar{N}_a\right). \qquad (20)$$

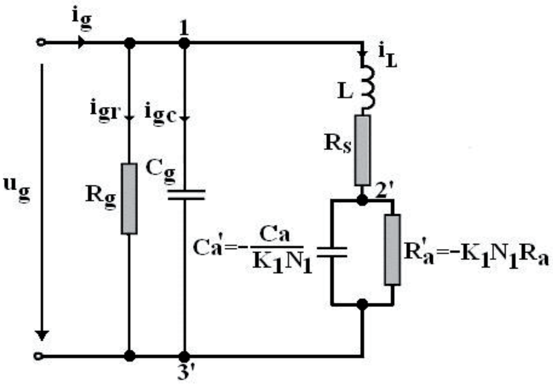

Fig. 5. Electrical small signal equivalent circuit for a BLD. R_g and R_a' are modified diffusion resistances, C_g and C_a' are modified diffusion capacitances for the generation and absorption region, respectively, L is an inductance, R_s is a damping resistance, K_1 and N_1 are constants, u_g, i_g, i_{gr}, i_{gc} and i_L are small signal voltages and currents at the gain section, respectively, m_g and m_a are technological constants [4].

5. The Condition for Bistability and the Basic Parameters of the Hysteresis Loop

To determine the condition for a bistable mode to occur in a BLD, we made the mathematical analysis for finding the extremes of function $I_g = g_1(N_{ph})$ was carried out. This function we derived by solution of rate equations (1) to (3) under the assumption that the lifetime of the carriers in generation as well as absorption regions τ_g, τ_a is not a function of the carrier concentration and the coefficient $\beta \approx 0$ [8], [9].

$$\frac{I_g}{I_{gth}} = \frac{x^3 + \left[1 + C + A(1+B) - \beta(AB + C) + \beta K\right]x^2}{A(1+B+C)(x+\beta A)(x+1)} + \frac{\left[A\left(1+B+C-\beta(B+C)-K\right)-\beta K\right]x - A\beta K}{A(1+B+C)(x+\beta A)(x+1)}, \qquad (21)$$

$$A = \left(g_g \tau_g N_{phs}\right)^{-1}, \qquad (22)$$

$$B = \alpha_1 g_g N_{og} \tau_{ph}, \quad (23)$$

$$C = \alpha_2 g_a N_{oa} \tau_{ph}, \quad (24)$$

$$x = \frac{N_{ph}}{N_{phs}}, \quad (25)$$

$$K = \frac{\alpha_2 \tau_{ph} I_a}{N_{phs} e V_a}. \quad (26)$$

We have analyzed function (21) under the condition $\beta = K = 0$. Equation (27) was differentiated and its roots were found revealing two real local extrema (28) – a minimum and a maximum.

$$x^2 + 2x + [1 + C(1 - A)] = 0, \quad (27)$$

$$x_{1,2} = \pm[C(A-1)]^{1/2} - 1. \quad (28)$$

By applying formulas (22), (24) and (25) we express (29) as

$$\Delta N_{ph2} = N_{ph2} - N_{ph\min} = N_{phs}\left[\left(g_a N_{oa} \tau_{ph} \alpha_2 \left(\frac{g_a \tau_a}{g_g \tau_g} - 1\right)\right)^{1/2} - 1\right]. \quad (29)$$

provided that $\Delta N_{ph1} = N_{ph\max} - N_{ph1}$; $x_1 = N_{ph2}$ and $N_{ph1} = N_{ph\min} = 0$. By use (28) we determine maximum (30) and minimum (31) of function (21)

$$I_{g\max} = I_{gth} = \frac{eVN_{phs}}{\tau_{ph}} A(1 + B + C), \quad (30)$$

$$I_{g\min} = \frac{eVN_{phs}}{\tau_{ph}}\left[A(1+B) + C + 2[C(A-1)]^{1/2} - 1\right], \quad (31)$$

$$\Delta I_{gh} = I_{g\max} - I_{g\min}. \quad (32)$$

The parameters of the hysteresis loop ΔI_{gh} and ΔN_{ph} is connected with points B, C and D (see Fig. 6) and are simply related as follows

$$\Delta I_{gh} = \frac{eV}{g_a \tau_a \tau_{ph}} (\Delta N_{ph})^2. \quad (32)$$

The measured and simulated parameters of the light-current characteristic hysteresis loop are shown in Tab. 3, the values of the physical constants are specified in Tab. 4.

	ΔP [mW]	ΔI_{gh} [mA]
Measured	5.6	14
Simulated	5.2	16

Tab. 3. The measured and simulated parameters of the light-current hysteresis loop.

From extreme analysis of function (21) the condition for origination of a BLD bistability mode after (27), (28) has the following form

$$[C(A-1)] > 1. \quad (34)$$

This can be expressed as

$$\frac{R_a}{R_{ac}} > 1 \quad (35)$$

where R_a is the rate of photon absorption in the saturable absorption centers in the absorption regions expressed by (36), and R_{ac} is the critical photon absorption rate at the non-saturable centers in the absorption regions of a multiple-divided strip contact determined by relation (37). This condition can be expressed by stating that non-linear behavior of the two areas must be distinct enough from each other and that the origination of a LD bistable mode must be conditioned by the fact that the photon absorption rate at the saturable absorption centers must be greater than the absorption rate caused nonsaturable optical losses.

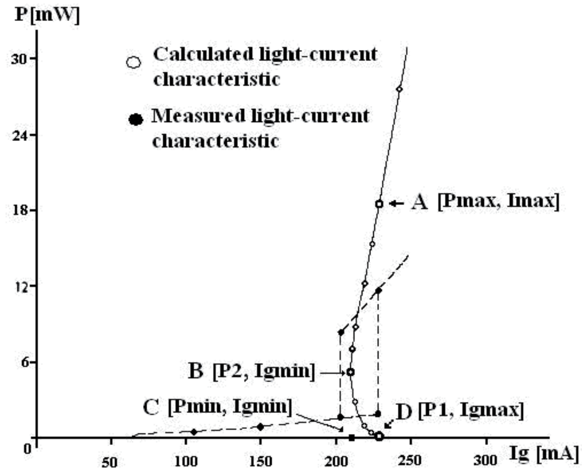

Fig. 6. Measured and calculated light-current characteristic of a BLD. ($P = k N_{ph}$, k=8.7 ·10^{-17} [W; cm^{-3}; W/ cm^{-3}]).

g_g [cm^3·s^{-1}]	g_a [cm^3·s^{-1}]	N_{og} [cm^{-3}]
8·10^{-7}	6·10^{-6}	9·10^{17}
τ_g [s]	τ_a [s]	N_k [cm^{-3}]
2.2·10^{-9}	1.1·10^{-8}	5.9·10^{17}
N_{oa} [cm^{-3}]	τ_{ph} [s]	B [cm^3·s^{-1}]
2.5·10^{17}	2.2·10^{-12}	1.3·10^{-10}
V [cm^3]	β [-]	α_2 / α_1 [-]
1.5·10^{-9}	0	0.25

Tab. 4. Optimized value of the physical constant for light-current hysteresis loop modeling.

By substituting relations (36) and (37) into inequality (39) it is possible to determine the minimal size of the absorption area α_{2k}. This area is needed for the creation of a bistable mode in an LD according to relation (38). The average calculate value was α_{2k} = 0.0084.

$$R_a = g_a N_{oa}, \quad (36)$$

$$R_{ac} = \left[\left(\frac{g_a \tau_a}{g_g \tau_g} - 1\right)\tau_{ph} \alpha_2\right]^{-1}, \quad (37)$$

$$\alpha_{2k} = \left[g_a N_{oa} \tau_{ph} \left(\frac{g_a \tau_a}{g_g \tau_g} - 1 \right) \right]^{-1}. \tag{38}$$

An extremes analysis of function (21) also provides the other necessary condition for the occurrence of a bistable mode in an LD (39) that could be called a condition for Q-switching taking place e.g. in self-pulsating lasers.

$$\frac{g_a \tau_a}{g_g \tau_g} > 1. \tag{39}$$

This condition applies generally to creation of dynamic instabilities in the radiation of semiconductor laser diodes such as permanent self-pulsation or bistability [9].

6. Conclusion

A mathematical model for bistable laser diode - BLD was created using the system of three rate equations and derived the relationship for the light-current characteristic. The model uses physical constants the values of which were determined by methods employing modulation and optimized by simulation. A BLD was designed and confirmed that the presence of inhomogeneous excitation caused by nonuniform contacts can produce bistability in the output radiation of BLD. A simple model is analyzed which displays the main features of semiconductor laser with inhomogeneous current injection – BLD, namely a hysteresis in the light current characteristic and negative resistance and capacitance, which is optoelectronic in origin across the absorber sections. A small signal analysis of this model leads to an electrical equivalent circuit which clarifies the frequency limitations of the device up to several hundred megahertz.

The physical constants values of the model were optimized in relation to the measured values of the static light-current characteristic $I_{gth,}$ ΔI_{gh} and ΔP. The comparison of measured and optimized light current function is presented in Fig. 6. The optimized values of physical constants are shown in Tab. 1. For selected points P_1, P_2, $P_{\max}$ the elements of the small signal equivalent electrical circuit depicted in Fig. 5 are given in Tab. 2. The circuit elements $R_a{}'$ and $C_a{}'$ characterizing the influence of absorption areas have negative values. This means that the BLD produces unstable radiation in an area of excitation evident in its light-current characteristics. The small signal equivalent electrical circuit contains only negative $R_a{}'$ for the self-pulsation type instability of the LD. The bistable mode can only exist when a sufficiently large negative $C_a{}'$ capacitance is present in addition to the negative $R_a{}'$. If this capacitance is not large enough, the device pulsates with a frequency represented by the L and C_g values.

BLD is a perspective element; it can be used as an electro-optical limiter, a simple logic device and an optical memory element. However, its direct use in practice is hindered by some problems. The higher threshold current and strong temperature dependence of the bistable mode prevented the introduction of continuous bistable operating mode in the prepared samples.

Acknowledgements

This work was supported by the Czech Science Foundation and was carried out in the framework of research project No.102/06/0424 and research project MSM 6840770014 of the Czech Technical University in Prague.

References

[1] LASHER, G. J. Analysis of proposed bistable injection lasers. *Solid-State Electronics,* 1964, vol. 7, no. 11, p. 707 - 716.

[2] BASOV, N. G. 0 – 1 Dynamics of injection lasers. *IEEE J.Quantum Electron.*, 1968, vol. 4, no.11, p. 855 - .864.

[3] LEE, T. P., ROLAND R. H. Repetitively Q – switched light pulses from GaAs injection lasers with tandem double section stripe geometry. *IEEE J. Quantum Electron.*, 1970, vol. 6, no. 6, p. 339 – 350.

[4] HARDER, C., LAU, K., YARIV, A. Bistability and pulsations in semiconductor lasers with inhomogenous current injection. *J. Quantum Electronics*, 1982, vol. 18, no.9, p. 1351 - 1361.

[5] KAWAGUCHI, H., IWANE, G. Bistable operation in semiconductor lasers with inhomogenous excitation. *Electron. Letters*, 1991, vol. 17, no.4, p. 167- 168.

[6] JEŘÁBEK, V, HŰTTEL, I. Bistability of the laser diode with a multiple-divided contact stripe. In *Proceedings of SPIE, Lasers and Application*s. Warsaw (Poland), 2005, p. 595821-1 – 9.

[7] PEGG, S. I., ADAMS, M. J., POGUNTKE, K. Simultaneous absorptive and dispersive all-optical switching of a section bistable laser diode. *Optics Communications*, 2002, vol. 174, no. 1-4, p. 191-194.

[8] TAKENAKA, M., NAKANO Y. All-optical flip-flop multimode interference bistable laser diode. *IEEE Photonics Technology Letters*, 2005, vol. 17, no.5, p. 968-970.

[9] PISARCHIK, A. N., KUNSEVITCH, B. F. Control of multistability in a directly modulated diode laser. *IEE J. Quantum Electronics,* 2002, vol. 38, no.12, p. 1594-1598.

[10] UENO, M., LANG, R. Condition for self-sustained pulsation and bistability in semiconductor lasers. *J. Applied Physics,* 1985, vol. 58, no.4, p. 1689 - 1692.

[11] HILL, M. T., WAARDT, H., KHOE, G. D. All-optical flip-flop based on coupled laser diodes. *IEEE J. Quantum Electronics*, 2008, vol. 37, no.3, p. 405-413.

About Authors

Vítězslav JEŘÁBEK was born in Prague 1951. He received his M.Sc and PhD in the Microelectronics from the Czech Technical University (CTU) in Prague 1975, and 1987. From 2005 is head of optoelectronics group at the Dept. of Microelectronics, CTU. His research interests include planar hybrid integrated optics and optoelectronics

devices, modules and systems design, technology and measuring.

Ivan HÜTTEL was born in Prague 1938. He received his PhD degree from the Czech Technical University, Faculty of Electrical Engineering, Prague in 1968, the DSc. degree from the Institute of Radiocommunications and Electronics in 1990 and Assoc. Prof. at the Institute of Chemical Technology, Prague in 1989. His research activities are physics of thin films, technology of semiconductor lasers and integrated optics, photonics polymer structures.

RADIOENGINEERING REVIEWERS III

June 2011, Volume 20, Number 2

- NOVOTNÝ, V., Brno Univ. of Technology, Czechia
- PÁTA, P., Czech Technical University in Prague, Czechia
- PIKSA, P., Czech Technical University in Prague, Czechia
- POLÁK, L., Brno Univ. of Technology, Czechia
- POLÍVKA, M., Czech Technical University in Prague, Czechia
- PROKEŠ, A., Brno Univ. of Technology, Czechia
- PROKOP, R., Brno Univ. of Technology, Czechia
- RABOCH, J., Czech Technical University in Prague, Czechia
- RAIDA, Z., Brno Univ. of Technology, Czechia
- ROVŇÁKOVÁ, J., Technical University of Košice, Slovakia
- RUPP, M., Vienna University of Technology, Austria
- ŘÍHA, K., Brno Univ. of Technology, Czechia
- SCHEJBAL, V., University of Pardubice, Czechia
- SCHWARZ, D., Masaryk University, Czechia
- SEGOVIA-VARGAS, D., Carlos III University of Madrid, Spain
- SENANI, R., Netaji Subhas Institute of Technology, New Delhi, India
- SIZOV, V., University of Birmingham, UK
- SLANINA, M., Brno Univ. of Technology, Czechia
- SMÉKAL, Z., Brno Univ. of Technology, Czechia
- SOLIMAN, A., Cairo University, Egypt
- SIRIPRUCHYANUN, M., King Mongkut's Univ. of Technology North Bangkok, Thailand
- STAMENOV, P., T-Mobile CZ, Czechia
- SYSEL, P., Brno Univ. of Technology, Czechia
- SZABÓ, Z., Czech Technical University in Prague, Czechia
- ŠEBESTA, J., Brno Univ. of Technology, Czechia
- ŠEBESTA, V., Brno Univ. of Technology, Czechia
- ŠIMŠA, J., Academy of Sciences of the Czech Republic, Czechia
- ŠKVOR, Z., Czech Technical University in Prague, Czechia
- ŠOTNER, R., Brno Univ. of Technology, Czechia
- TANGSRIRAT, W., King Mongkut's Institute of Technology Ladkrabang (KMITL), Thailand
- TSIVIDIS, Y., Columbia University, New York, USA
- ULOVEC, K., Czech Technical University in Prague, Czechia
- URBANEC, T., Brno University of Technology, Czechia
- VACULÍK, M., University of Zilina, Slovakia
- VALENTA, V., ESIEE Paris, France
- VALSA, J., Brno Univ. of Technology, Czechia
- VARGIČ, R., Slovak University of Technology, Bratislava, Slovakia
- VILOVIĆ, I., University of Dubrovnik, Croatia
- VODRÁŽKA, J., Czech Technical University in Prague, Czechia
- VOZŇÁK, M., VŠB - Technical University of Ostrava, Czechia
- WILFERT, O., Brno University of Technology, Czechia
- WINAI, J., Suan Sunandha Rajabhat University, Thailand
- YILMAZ, A. E., Ankara University, Turkey
- ZHANG, H., Zhejiang University, China
- ZHANG, L., Harbin Institute of Technology, China
- ZHANG, N., University of Florida and Maxlinear Inc., USA
- ZVÁNOVEC, S., Czech Technical University in Prague, Czechia